

ORIGINAL RESEARCH

A target anti-occlusion method based on image processing and trajectory prediction in electro-optical tracking system

Wenqiang Xia^{1,2,3}  | Qianwen Duan^{1,2,3} | Jiuqiang Deng^{1,2,3} | Yao Mao^{1,2,3} 

¹Institute of Optics and Electronics, Chinese Academy of Sciences, Chengdu, China

²Key Laboratory of Optical Engineering, Chinese Academy of Sciences, Chengdu, China

³Chinese Academy of Science, Beijing, China

Correspondence

Yao Mao, Institute of Optics and Electronics, Chinese Academy of Science, Chengdu 610209, China.

Email: maoyao@ioe.ac.cn

Funding information

National Natural Science Foundation of China, Grant/Award Numbers: 61733012, 61905253

Abstract

In the electro-optical tracking system, due to the full occlusion of clouds or buildings, the traditional tracking algorithm fails to work effectively. In the authors' study, a dual-channel anti-occlusion scheme based on image processing and trajectory prediction is proposed. On the one hand, the image-processing unit plays a significant role in evaluating the occlusion state of the target. An improved image occlusion judgement method based on Bhattacharyya coefficient occlusion judgement is proposed, and the ability to resist background interference and rapidity of the algorithm is enhanced. On the other hand, according to the different occlusion states, the dual operation modes of tracking and prediction are usually set. When the target is completely occluded, the prediction mode based on a robust predictive filtering method is investigated to predict the real-time trajectory of the target more accurately. Image occlusion judgement and trajectory prediction can solve the occlusion problems in tracking control. Otherwise, the feasibility and effectiveness of the proposed method are verified by experiments.

KEY WORDS

anti occlusion, electro-optical tracking system, image occlusion judgement, robust predictive filtering, trajectory prediction

1 | INTRODUCTION

Target tracking technology is widely used in military guidance [1, 2], virtual reality [3], video surveillance [4], medical diagnosis [5], robot control [6] and other scientific fields. Target occlusion has always been one of the most challenging problems in target tracking [7, 8]. In the electro-optical tracking system, target tracking means that the line of sight (LOS) of the system follows the target [9]. The first step in the tracking process is detecting the target by an image sensor. The second step is calculating the LOS error by the image processing unit. The last step is executing a closed-loop control law based on the LOS error. Figure 1 shows the tracking principle of electro-optical tracking systems. However, tracking failures are more likely to occur when the target is occluded. For example, the false targets or obstacles are extracted as well as the target is out of the field of vision.

In the published references, some image tracking algorithms are suitable for the occlusion problem. The target

tracking algorithm based on MeanShift [10, 11] can solve the partial occlusion problem of the target. In Ref. [12], an interactive particle filter method by analysing the occlusion relationship between different targets was proposed and successfully resolved the mutual occlusion problem in tracking multi-pedestrians. In Ref. [13], a novel occlusion-handling tracker is proposed based on the discriminative correlation filters framework. It followed a hybrid approach to handle partial occlusion and full occlusion. However, these image processing algorithms all track the target in the dynamic image sequence. In general, for electro-optical tracking systems, the target needs to be located in the centre of the field of view of the image sensor. This requires both the image processing unit and the servo control unit to realise. Therefore, when the target is completely occluded, reliable tracking cannot be achieved by relying solely on the image tracking algorithm. On the other hand, when the target is completely occluded, the LOS error extracted by the image processing unit is invalid. If the controller is provided with the incorrect LOS error as the

This is an open access article under the terms of the Creative Commons Attribution License, which permits use, distribution and reproduction in any medium, provided the original work is properly cited.

© 2022 The Authors. *IET Radar, Sonar & Navigation* published by John Wiley & Sons Ltd on behalf of The Institution of Engineering and Technology.

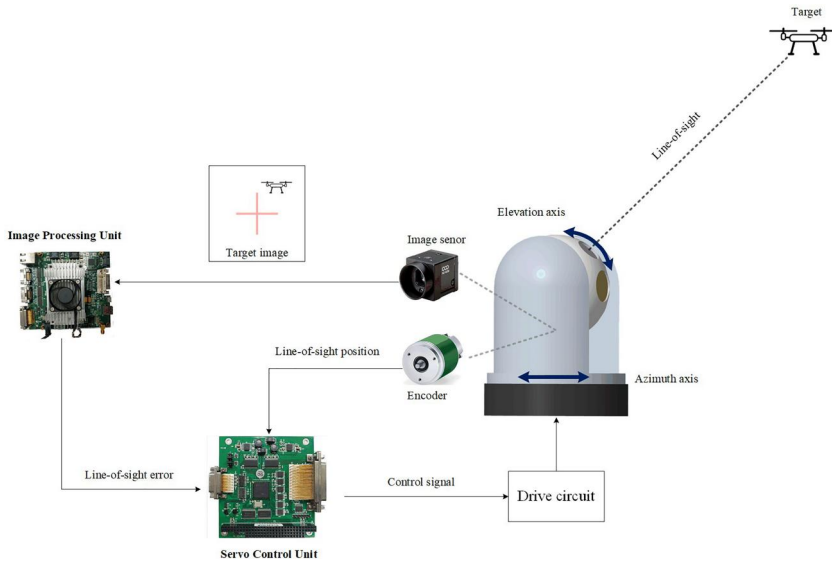


FIGURE 1 Tracking schematic of the electro-optical tracking system

tracking error to control the LOS, it will lead to tracking divergence. Therefore, it is an important task to judge whether the target is occluded and design a reasonable control strategy.

As for the target occlusion judgement method, there have been some studies before. In Ref. [14], the image correlation confidence was used to judge occlusion, but the calculation of image correlation confidence depends on target tracking, and it needs the exhaustive method for template matching in target tracking, resulting in higher computational complexity of the algorithm. In Ref. [15], the relative magnitude of probability density between the single feature target template and the candidate template was used, which is a more robust method for partial occlusion problems, but when the target is fully occluded, the occlusion judgement factor based on the single feature cannot judge accurately. In Ref. [16], the residual between the observed value of the target and the optimal estimate of the Kalman filter was used to judge whether the target was occluded or not, but the optimal estimate is related to the tracking algorithm, and the occlusion judgement is uncertain. In Ref. [17], the Kalman filter was introduced to reduce the iteration number of the mean shift algorithm, and the Bhattacharyya coefficient was proposed, which had low computational complexity, but there are shortcomings in both time and accuracy of judging occlusion.

To solve the stable tracking problem of electro-optical tracking systems under full occlusion, a dual-channel anti-occlusion scheme based on image processing and trajectory prediction is proposed. The main contributions or innovations are as follows:

- The LOS error is fused with the LOS position obtained by position sensors to obtain the angular position of the target, which are used for trajectory prediction
- An improved BCOJ method based on a background weighting factor is proposed, which can reduce the influence of background pixels on the traditional BCOJ method and improve the speed of occlusion judgement

- In the prediction mode, considering the time delay, model uncertainty, and variable prediction step size, robust predictive filtering has higher accuracy than that of traditional prediction methods

The rest of this paper is organised as follows: Section 2 elaborates on the proposed dual-channel anti-occlusion scheme based on image processing and trajectory prediction in more detail. Section 3 gives the improved method of target occlusion judgement and demonstrates the feasibility of the proposed scheme through experiments. Section 4 describes robust predictive filtering and simulation verification. Section 5 shows the experimental verification of the overall scheme. Section 6 summarises the innovation and shortcomings of this paper.

2 | OVERVIEW OF SCHEME

In terms of the stable tracking problem of the electro-optical tracking system under full occlusion, the schematic block diagram presented in this study is shown in Figure 2. Without considering occlusion, the image processing unit extracts the target and calculates the LOS error. The servo control unit only uses the LOS error for closed-loop control, and the servo control unit uses the LOS error to track the target. However, in the proposed scheme, the image processing unit also needs to provide the occlusion state information and the system needs an additional prediction controller to predict the target trajectory.

Realising the trajectory prediction needs the historical angular position of the target, but the image processing unit can only provide the LOS error. In this scheme, a method based on equivalent feed-forward control is introduced to acquire target angular position [12]. It solves the coupling of target tracking and image processing. In other words, the LOS error and the LOS position are fused to obtain the angular position of the target.

FIGURE 2 Block diagram of the anti-occlusion scheme based on image processing and trajectory prediction. LOS, line of sight

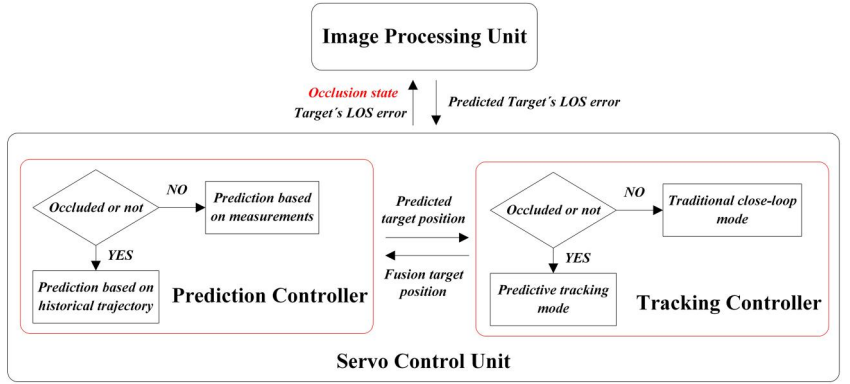


Figure 3 is a schematic diagram of a two-axis electro-optical tracking system. Because of the similarity of the two axes, the elevation axis (E axis) is mainly described. $\Delta\theta_{target}^E$ represents the LOS error obtained by the image processing unit on the E axis, $\theta_{platform}^E$ represents the LOS position obtained by position sensors, and θ_{target}^E is the angular position of the target. They can be written as follows:

$$\theta_{target}^E = \theta_{platform}^E + \Delta\theta_{target}^E \quad (1)$$

Due to the integration time of the image sensor, the processing time of the image processing unit, and the transmission time of the LOS error data, there is a non-negligible time delay in the LOS error obtained by the servo control unit. However, the time delay of the encoder for detecting the LOS position of the electro-optical tracking system is small and can be ignored. Therefore, it is necessary to manually delay the LOS position $\theta_{platform}^E$ of the electro-optical tracking system when synthesising the target position to ensure the time axis is aligned. It is expressed as:

$$\theta(k-d)_{target}^E = \theta(k-d)_{platform}^E + \Delta\theta(k)_{target}^E \quad (2)$$

In Equation (2), k represents the current moment, and d is the delayed frames of the image sensor. Since the synthesised target angular position information has time delay and fusion noise (time axis may not be aligned), the system needs to filter and predict it.

The servo control units are given in Figures 4 and 5 are provided with the tracking mode when the target is not occluded, and the prediction mode is adopted when the target is occluded. When the target is occluded, the LOS error extracted by the image-processing unit is no longer valid, and the tracking controller cannot continue to use the traditional closed-loop mode based on the LOS error. Therefore, in this paper, a dual-mode tracking controller based on the target occlusion state is used. When the target is occluded, the tracking controller selects the prediction mode, and the prediction step size will gradually increase until the occlusion state changes.

In Figure 4, R is the reference input signal of the system, Y is the output signal of the system and E represents the tracking error. Actually, since the image sensor can only extract the LOS

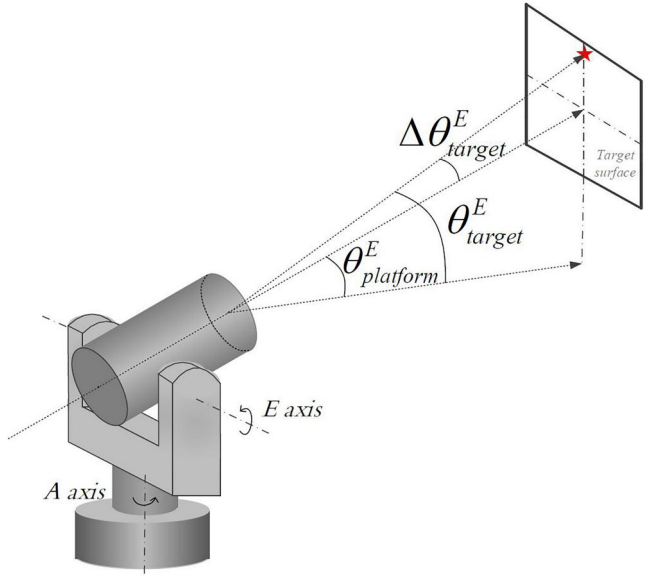


FIGURE 3 Schematic diagram of electro-optical tracking system

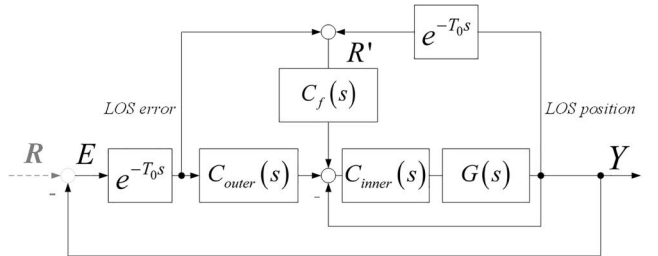


FIGURE 4 Tracking mode. LOS, line of sight

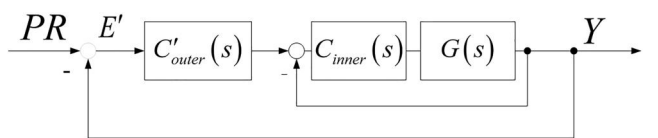


FIGURE 5 Prediction mode

error, R is an unknown data, so it is represented with the dashed line in the block diagram. Because there is a time delay when the image processing unit sends out a LOS error, the transfer characteristics ($e^{-T_{os}}$) of the image processing unit are shown in Figure 4. $G(s)$ represents the characteristics of the controlled object of the control system. $C_{outer}(s)$ and $C_{inner}(s)$ controllers represent the outer loop controller and the inner loop controller, respectively. The main purpose of the inner loop is to improve the linearity of the system. The tracking ability of the system is mainly determined by the outer loop. The feed-forward controller $C_f(s)$ is used to reduce the impact of LOS error's time delay on the tracking accuracy of the system.

In Figure 5, PR indicates the current angular position of the target predicted by historical trajectory. The LOS error does not need to be obtained from the image processing unit when the target is predicted, so the time required for this process is short and can be neglected. Therefore, there is no pure delay link $e^{-T_{os}}$ in the prediction mode, and a better controller in the outer loop can be redesigned. Besides, there are many predictive filtering methods, such as Standard Kalman Filter (SKF) [13], Extended Kalman Filter (EKF) [14], Unscented Kalman Filter (UKF) [15], Particle Filter (PF) [16] etc. These methods have their applicability and the corresponding predictive filtering methods can be selected according to different actual scenarios. In the proposed scheme, the prediction step size is required to change with the duration of the occlusion state, and the target motion model is uncertain, so the above tracking method is not applicable. Considering the time delay, model uncertainty, and variable prediction step size, robust predictive filtering is an excellent prediction algorithm, which can meet the needs of trajectory prediction in an electro-optical tracking system.

According to the above description of this scheme, the occlusion state information runs through the whole scheme. Therefore, to realise the scheme proposed in this paper, the most important thing is to provide a stable and rapid occlusion judgement method.

3 | TARGET OCCLUSION JUDGEMENT METHOD BASED ON IMPROVED BHATTACHARYYA COEFFICIENT WITH BACKGROUND WEIGHTING

The similarity measure-based occlusion judgement method, also known as the template matching method based on the Bhattacharyya coefficients, is initially used to measure the separability of two discrete probability distributions and is later used to approximate the overlap of two statistical samples. In tracing, a template matching method based on Bhattacharyya coefficients is used to calculate the similarity between the target and the initial template. In the process of entering occlusions, the similarity between the target and the initial target model decreases gradually. In the process of leaving from the occlusion, the target characteristic information is gradually recovered, and the target similarity value is gradually increased.

The occlusion judgement method based on the Bhattacharyya coefficient is the current mainstream occlusion judgement method, with low computational complexity and easy implementation. The Bhattacharyya coefficient is a template matching indicator of the image, which is used to measure the similarity between the target and the candidate model. However, the Bhattacharyya coefficient is susceptible to interference from background information and is unable to judge occlusion timely and accurately. Therefore, in this paper, an improved method based on background weighting is proposed to replace the occlusion judgement method based on the traditional Bhattacharyya coefficient.

3.1 | Theoretical derivation

First, the Bhattacharyya coefficient is defined as follows [17]:

$$\hat{p}(y) \equiv \rho[\hat{p}(y), \hat{q}] = \sum_{u=1}^m \sqrt{\hat{p}_u(y) \hat{q}_u} \quad (3)$$

In Equation (3), \hat{q} is a feature histogram of the real target, $\hat{p}(y)$ represents a feature histogram of the candidate target, and m is the number of the characteristic histogram group. \hat{q}_u and $\hat{p}_u(y)$ are defined, respectively, as follows:

$$\begin{aligned} \hat{q}_u &= C \sum_{i=1}^n k\left(\left\|\frac{x-x_i}{b}\right\|^2\right) \delta[b(x_i) - u] \\ C &= \frac{1}{\sum_{i=1}^n k\left(\left\|\frac{x-x_i}{b}\right\|^2\right)} \end{aligned} \quad (4)$$

$$\begin{aligned} \hat{p}_u(y) &= C_b \sum_{i=1}^{n_k} k\left(\left\|\frac{y-x_i}{b}\right\|^2\right) \delta[b(x_i) - u] \\ C_b &= \frac{1}{\sum_{i=1}^{n_k} k\left(\left\|\frac{y-x_i}{b}\right\|^2\right)} \end{aligned} \quad (5)$$

In Equation (4), \hat{q}_u represents the weight corresponding to the u th colour in the feature histogram of the real target, and x represents the position of the centre point of the real target image. In Equation (5), $\hat{p}_u(y)$ represents the weight corresponding to the u th colour in the feature histogram of the candidate target, and y represents the position of the centre point of the candidate target image. Then, the meaning of $\delta[b(x_i) - u]$ is not difficult to understand, if the colour of the pixel x_i is in the grouping interval of the u th colour ($b(x_i) = u$), $\delta[b(x_i) - u] = \delta(0) = 1$, otherwise, $\delta[b(x_i) - u] = 0$. n represents the number of regional pixel points of the real target image, n_k represents the number of regional pixel points of the candidate target image, and $k(\|x\|^2)$ represents the profile function corresponding to the kernel function $K(x)$. b represents the bandwidth factor. C , C_b is a normalised parameter, causing $\sum_{u=1}^m \hat{q}_u =$

$\sum_{u=1}^m \hat{p}_u(y) = 1$. Therefore, both $(\sqrt{\hat{p}_1(y)}, \sqrt{\hat{p}_2(y)}, \dots, \sqrt{\hat{p}_m(y)})$ and $(\sqrt{\hat{q}_1}, \sqrt{\hat{q}_2}, \dots, \sqrt{\hat{q}_m})$ are m -dimensional unit vectors, and the geometric meaning of the Bhattacharyya coefficient $\hat{\rho}(y) = \sum_{u=1}^m \sqrt{\hat{p}_u(y)\hat{q}_u}$ is the cosine of the angle between the m -dimensional unit vectors $(\sqrt{\hat{p}_1(y)}, \sqrt{\hat{p}_2(y)}, \dots, \sqrt{\hat{p}_m(y)})$ and $(\sqrt{\hat{q}_1}, \sqrt{\hat{q}_2}, \dots, \sqrt{\hat{q}_m})$ (it can also be called the inner product of the vector). The larger the cosine value in the range of 90° , the smaller the angle is, indicating the closer the two vectors are pointing. When $\hat{\rho}(y) = 1$, it indicates that the two-unit vectors coincide, and they are the most similar at this time. When $\hat{\rho}(y) = 0$, the two-unit vectors are orthogonal, and they are the most dissimilar. Therefore, the Bhattacharyya coefficient is also called the similarity between the candidate target image and the real target image.

In the process of image target tracking, the maximum value $\hat{\rho}(y)_{\max}$ of $\hat{\rho}(y)$ in each frame of image is found by the mean shift algorithm [10]. That is, a candidate target image that is most similar to the real target image is found. When the target is normally tracked, the value of the Bhattacharyya coefficient fluctuates within a certain range. However, when the target is occluded, the value of the Bhattacharyya coefficient drops sharply. Therefore, the Bhattacharyya coefficient can be used as the occlusion judgement method for image target tracking. First, the occlusion threshold is set as ρ_T . Then, $\hat{\rho}(y)_{\max}$ in the current frame of image is used to compare with the occlusion threshold ρ_T . When $\hat{\rho}(y)_{\max} > \rho_T$, it indicates that the target is not occluded. Otherwise, when $\hat{\rho}(y)_{\max} \leq \rho_T$, it indicates that the target is occluded.

Since the classical Bhattacharyya coefficient judgement method is susceptible to the background pixels, in this paper, an improvement based on the background weighting for the classical Bhattacharyya coefficient judgement is proposed. By establishing the background histogram in the annular region outside the target region, the weight derived from the log-likelihood ratio of the target histogram and the background histogram is used as the background weighting factor, and the background weighting factor is added to the target characteristic model to reduce the influence of the background pixels, thus improving the occlusion detection capability of the algorithm.

As shown in Figure 6 below, the red rectangle is the target area, the outer ring area of the target is the background area, and the histogram model of the background area is defined by Equation (6).

$$B_u = \sum_{i=1}^{n_k} \delta[b(x_i) - u]/n_k \quad (u = 1, 2, \dots, m) \quad (6)$$

Then, the log-likelihood ratio of the colour value u is calculated as follows:

$$L_u = \lg \frac{\max\{q_u, \eta\}}{\max\{B_u, \eta\}} \quad (u = 1, 2, \dots, m) \quad (7)$$

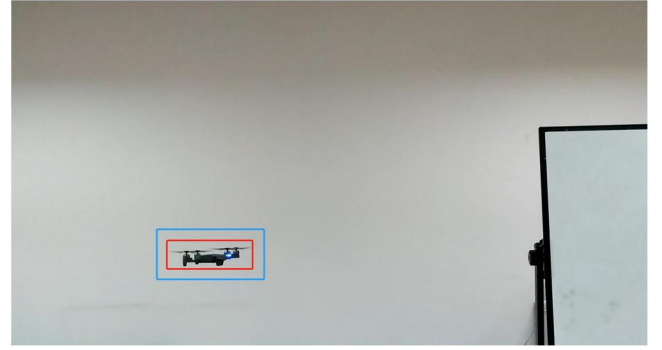


FIGURE 6 Histogram modelling of background

In Equation (7), η is used to prevent q_u and B_u from being 0 (an error), so η is assigned a small value (0.1×10^{-6}). In the above formula, if a colour u has a larger proportion in the target image than in the background image, then $L_u > 0$. If it has the same proportion in the target image and the background image, then $L_u = 0$. If it has less proportion in the target image than in the background image, then $L_u < 0$.

Next, the background weighting coefficient is calculated. When $L_u > 0$, it indicates that the proportion of the colour u in the target image is larger than that in the background image. Therefore, for such a colour, our background weight should be relatively large. The larger the ratio of the two proportions is, the larger the background weight should be. When $L_u < 0$, it means that the proportion of the colour u in the target image is smaller than that in the background image. For such a colour, the background weight should be smaller. The smaller the ratio of the two proportions is, the smaller the background weight should be.

According to the log-likelihood ratio value obtained by Equation (7), the background weighting coefficient is obtained as:

$$\mu_u = \begin{cases} a + \frac{L_u}{L_{\max}} \times (1-a) & L_u > 0 \\ a & L_u = 0 \ (u = 1, 2, \dots, m) \\ \frac{L_{\min} - L_u}{L_{\min}} \times (1-a) & L_u < 0 \end{cases} \quad (8)$$

where a represents the background scale factor of the background weighting factor ($0 \leq a < 1$).

Correspondingly, the target feature histogram based on background weighting is described as follows:

$$\begin{aligned} \hat{q}'_u &= C' \sum_{i=1}^n \mu_u k\left(\left\|\frac{x-x_i}{b}\right\|^2\right) \delta[b(x_i) - u] \\ C' &= \frac{1}{\sum_{i=1}^n \mu_u k\left(\left\|\frac{x-x_i}{b}\right\|^2\right)} \end{aligned} \quad (9)$$

The improved Bhattacharyya coefficient based on background weighting can be described by Equation (10):

$$\begin{aligned}
\hat{\rho}'(y) &\equiv \rho[\hat{p}(y), \hat{q}'] \\
&= \sum_{u=1}^m \sqrt{\hat{p}_u(y) \hat{q}'_u} \\
&= \sum_{u=1}^m \sqrt{\hat{p}_u(y) \cdot C' \sum_{i=1}^n \mu_u k \left(\frac{\|x - x_i\|^2}{b} \right) \delta[b(x_i) - u]}
\end{aligned} \tag{10}$$

The occlusion state is judged by using the improved Bhattacharyya coefficient based on background weighting. The workflow is consistent with that of the occlusion judgement method of the classical Bhattacharyya coefficient. The occlusion judgement method of the improved Bhattacharyya coefficient with background weighting can reduce the influence of the background pixels on occlusion judgement, thus improving the occlusion detection capability of the algorithm.

3.2 | Experimental verification

In this paper, a group of unmanned aerial vehicles is controlled to encounter the image sequence of the occlusion object with similar background colour, to carry out image tracking of the targets. The image target tracking method is the Meanshift algorithm [10]. The acquisition of video images and the video frames is finished by DirectShow, and the image rendering and subsequent image tracking processing are completed by OpenCV. In terms of hardware, the type of video collection card is Ospery-460e and video images are transmitted through the PCI-E interface. In the process of tracking, the traditional Bhattacharyya coefficient and the improved Bhattacharyya coefficient based on background weighting are calculated simultaneously. The effectiveness of the target occlusion judgement method based on the improved Bhattacharyya coefficient with background weighting is verified by comparative analysis.

Figure 7 shows the comparison of the traditional Bhattacharyya coefficient and the improved Bhattacharyya coefficient with background weighting. In Figure 7, the traditional Bhattacharyya coefficient is represented by a solid blue line. When the target is occluded, its value is stabilised at around 0.6646. If $\rho_T = 0.5$, then $\hat{\rho} > \rho_T$, and in the traditional Bhattacharyya coefficient occlusion judgement method the target is considered not occluded at this time, so the traditional occlusion judgement method fails. In addition, in Figure 7, the improved Bhattacharyya coefficient with background weighting is indicated by a red dotted line. When the target is occluded, the value is stabilised at around 0.3778. If $\rho_T = 0.5$, then $\hat{\rho} < \rho_T$, and in the traditional occlusion judgement method of Bhattacharyya coefficient with background weighting, the target is considered occluded at this time, so the improved occlusion judgement method is considered to be successful in occlusion judgement. The experimental results show that the proposed occlusion judgement method of the improved Bhattacharyya coefficient with background weighting can effectively enhance the occlusion judgement ability of the system, especially when the background colour of the target is similar to that of the occlusion

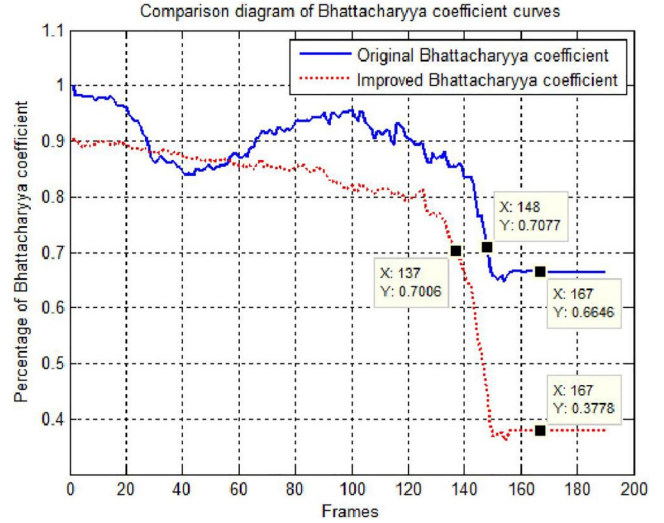


FIGURE 7 Comparison between the traditional Bhattacharyya coefficient curve and improved Bhattacharyya coefficient curve

object. On the other hand, if we assume that $\rho_T = 0.7$, according to the above analysis, the above two occlusion judgement methods can succeed in occlusion judgement, but the improved occlusion judgement method succeeds 11 frames earlier than the traditional occlusion judgement method. This shows that the occlusion judgement method of the improved Bhattacharyya coefficient can not only reduce the interference of background pixels but also improve the rapidity of the algorithm. Then, the improved occlusion judgement method is also beneficial to raise the response speed of the servo control unit for target occlusion.

4 | ROBUST PREDICTIVE FILTERING

4.1 | Theoretical analysis

When the occlusion state is obtained, it is important to choose a predictive algorithm to predict the trajectory of the target. This keeps the target in the centre of the field of view as much as possible. Once the target leaves the obstruction, the image algorithm can quickly extract the real target. Considering the time delay, model uncertainty, and variable prediction step size, robust predictive filtering is more accurate than traditional tracking methods.

First, assuming that the time delay is fixed, we can use an augmented delay-free model to realise robust prediction filtering. The following state-space model is proposed to describe the target characteristics of parameter uncertainty and fixed measurement delay.

$$\begin{cases} x_{k+1} = A_k(\varepsilon_k)x_k + B_k(\varepsilon_k)w_k \\ y_k = C_{k-d}(\varepsilon_{k-d})x_{k-d} + v_k \end{cases} \tag{11}$$

where $x_k \in \mathbb{R}^n$ is the state vector, $y_k \in \mathbb{R}^m$ is the measurement vector, and d is the frames of the measurement delay. The modelling errors ε_k are composed of L real-valued bounded scalars $\varepsilon_{i,k}$, $i = 1, \dots, L$. $A_k(\varepsilon_k)$, $B_k(\varepsilon_k)$, $C_k(\varepsilon_k)$ are matrices related to ε_k and of size $n \times n$, $n \times n$, $m \times n$. $w_k \in \mathbb{R}^n$ and

$v_k \in \mathbb{R}^m$ are uncorrelated and Gaussian random noise with variances Q and R , respectively.

$$\begin{cases} E[w_k w_j^T] = \delta_{kj} Q \geq 0 \\ E[v_k v_j^T] = \delta_{kj} R \geq 0 \\ E[w_k v_j^T] = 0 \end{cases} \quad (12)$$

The System (11) can be equivalently reconstructed into a delay-free System (13).

$$\begin{cases} \bar{x}_{k+1} = \bar{A}_k(\varepsilon_k) \bar{x}_k + \bar{B}_k(\varepsilon_k) w_k \\ y_k = \bar{C}_k(\varepsilon_k) \bar{x}_k + v_k \end{cases} \quad (13)$$

where, $\bar{x}_k = [x_k^T, \Delta_k^T, \Delta_{k-1}^T, \dots, \Delta_{k-d+1}^T]^T$, $\Delta_k = C_{k-1}(\varepsilon_{k-1}) x_{k-1} - C_k(\varepsilon_k) x_k$

$$\begin{aligned} \bar{A}_k(\varepsilon_k) &= \begin{bmatrix} A_k(\varepsilon_k) & \mathbf{0} & \mathbf{0} \\ C_k(\varepsilon_k) - C_{k+1}(\varepsilon_{k+1}) A_k(\varepsilon_k) & \mathbf{0} & \mathbf{0}_m \\ \mathbf{0} & I_{(d-1)m} & \mathbf{0} \end{bmatrix} \\ \bar{B}_k(\varepsilon_k) &= \begin{bmatrix} B_k(\varepsilon_k) \\ -C_{k+1}(\varepsilon_{k+1}) B_k(\varepsilon_k) \\ \mathbf{0}_{(d-1)m \times n} \end{bmatrix} \\ \bar{C}_k(\varepsilon_k) &= \begin{bmatrix} C_k(\varepsilon_k), \overbrace{I_m, \dots, I_m}^d \end{bmatrix} \end{aligned} \quad (14)$$

problems. One is the increase of calculation amount; the other is that with the increase of prediction length, the proportion of x_k in \bar{x}_k will decrease, so the accuracy of estimation will decrease. Therefore, it is more suitable for the short and fixed prediction step size.

After converting System (13) to an augmented delay-free model, the random parametric uncertainties of the target movement model are considered. A clear explanation of the SKF is to solve a regularised least squares (RLS) problem, which is presented in Equation (15).

$$\begin{aligned} &\begin{pmatrix} \hat{x}_{k|k+1} \\ \hat{w}_{k|k+1} \end{pmatrix} \\ &= \underset{\bar{x}_k, w_k}{\operatorname{argmin}} \left[\|x_k - \hat{x}_{k|k}\|_{P_{k|k}^{-1}}^2 + \|w_k\|_{Q_k^{-1}}^2 + \|y_{k+1} - \bar{C}_{k+1}(\varepsilon_{k+1}) \bar{x}_{k+1}\|_{R_{k+1}^{-1}}^2 \right] \end{aligned} \quad (15)$$

Here $\|x\|_W = \sqrt{x^T W x}$, x is a vector, and W is a positive definite matrix. Considering the estimation performance deterioration caused by modelling errors, the cost function of the RLS problem is improved as follows:

$$\begin{aligned} J(\alpha_k) &= E \left\{ \|\bar{x}_k - \hat{x}_{k|k}\|_{P_{k|k}^{-1}}^2 + \|w_k\|_{Q_k^{-1}}^2 + \|y_{k+1} - \bar{C}_{k+1}(\varepsilon_{k+1}) \bar{x}_{k+1}\|_{R_{k+1}^{-1}}^2 \right\} \\ &= \|\alpha_k\|_{\Phi_k}^2 + E \left\{ \|H_k(\varepsilon_k, \varepsilon_{k+1}) \alpha_k - \beta_k(\varepsilon_k, \varepsilon_{k+1})\|_{\Psi_k}^2 \right\} \end{aligned} \quad (16)$$

Remark 1 The advantage of the above-mentioned equivalent transformation is that the state-space model with measurement delay is equivalent to a state-space model without delay, which is conducive to the further design and implementation of the filter. At the same time, it can be seen from the expression of \bar{x}_k that the first element of \bar{x}_k is x_k , which means that if we use Equation (13) to estimate \bar{x}_k , we can get the expected estimated value of x_k . The advantage of this method is that it can predict the current state without multiple iterations. However, the expansion of the state vector dimension will lead to two

Here,

$$\begin{cases} \Psi_k = R_{k+1}^{-1} \\ H_k(\varepsilon_k, \varepsilon_{k+1}) = \bar{C}_k(\varepsilon_{k+1}) [\bar{A}_k(\varepsilon_k) \quad \bar{B}_k(\varepsilon_k)] \\ \beta_k(\varepsilon_k, \varepsilon_{k+1}) \\ \Phi_k = \operatorname{diag} \{ P_{k|k}^{-1}, Q_k^{-1} \} \\ \alpha_k = \operatorname{col} \{ \bar{x}_k - \hat{x}_{k|k}, w_k \} \end{cases} \quad (17)$$

According to the definitions of Φ_k and Ψ_k , the cost function $J(\alpha_k)$ is a strictly convex function. That is, there is a global minimum α_{kopt} at $\partial J(\alpha_k)/\partial \alpha_k = 0$. Find the partial derivative of Equation (16) for α_k and let $\partial J(\alpha_k)\partial \alpha_k = 0$, one obtains

$$\begin{aligned} & \left(\Phi_k + E \left\{ H_k(\epsilon_k, \epsilon_{k+1})^T \Psi_k H_k(\epsilon_k, \epsilon_{k+1}) \right\} \right) \alpha_k \\ &= E \left\{ H_k(\epsilon_k, \epsilon_{k+1})^T \Psi_k \beta(\epsilon_k, \epsilon_{k+1}) \right\} \end{aligned} \quad (18)$$

$$\left\{ \begin{array}{l} \hat{P}_{k|k} = \left(P_{k|k}^{-1} + G_{k11} \right)^{-1} \\ \hat{Q}_k = \left(Q_k^{-1} + G_{k22} - G_{k12}^T \hat{P}_{k|k} G_{k12} \right)^{-1} \\ \hat{\bar{B}}_k(0) = \bar{B}_k(0) - \bar{A}_k(0) \hat{P}_{k|k} G_{k12} \\ \hat{\bar{A}}_k(0) = \left(\bar{A}_k(0) - \hat{\bar{B}}_k(0) \hat{Q}_k G_{k12}^T \right) \\ \times \left(I_{n+md} - \hat{P}_{k|k} G_{k11} \right) \end{array} \right. \quad (22)$$

$$\begin{aligned} H_{k1} &= E \left\{ \begin{bmatrix} \bar{A}_k^T(\epsilon_k) \\ \bar{B}_k^T(\epsilon_k) \end{bmatrix} \bar{C}_{k+1}^T(\epsilon_{k+1}) R_{k+1}^{-1} \bar{C}_{k+1}(\epsilon_{k+1}) \times [\bar{A}_k(\epsilon_k) \bar{B}_k(\epsilon_k)] \right\} \\ H_{k2} &= E \left\{ \begin{bmatrix} \bar{A}_k^T(\epsilon_k) \\ \bar{B}_k^T(\epsilon_k) \end{bmatrix} \bar{C}_{k+1}^T(\epsilon_{k+1}) \right\} \\ H_{k3} &= E \left\{ \begin{bmatrix} \bar{A}_k^T(\epsilon_k) \\ \bar{B}_k^T(\epsilon_k) \end{bmatrix} \bar{C}_{k+1}^T(\epsilon_{k+1}) R_{k+1}^{-1} \bar{C}_{k+1}(\epsilon_{k+1}) \times \bar{A}_k(\epsilon_k) \right\} \end{aligned} \quad (19)$$

Obviously, $H_{k3} = H_{k1} [I_{(n+dm)} \ 0_{(n+dm) \times n}]'$.

Equation (18) has a similar form to Equation (12) in Ref. [18], so the recursive programme of the filter proposed in this paper can be further obtained. Because the derivation process is similar, it is omitted here.

The recursive procedure is composed of three steps. The first step is initialisation.

$$\left\{ \begin{array}{l} \hat{\bar{x}}_{0|0} = P_{0|0} E \{ \bar{C}_0(\epsilon_0) \} R_0^{-1} y_0 \\ P_{0|0} = \left(\bar{\Pi}_0^{-1} + E \{ \bar{C}_0^T(\epsilon_0) R_0^{-1} \bar{C}_0(\epsilon_0) \} \right)^{-1} \end{array} \right. \quad (20)$$

is presented, where

$$\bar{\Pi}_0 = E \left\{ (\bar{x}_0 - E(\bar{x}_0)) (\bar{x}_0 - E(\bar{x}_0))^T \right\}$$

The second step is parameter modification. A matrix is defined as

$$\begin{aligned} G_k &\triangleq H_{k1} - \begin{bmatrix} \bar{A}_k^T(0) \\ \bar{B}_k^T(0) \end{bmatrix} \bar{C}_{k+1}(0) R_{k+1}^{-1} \bar{C}_{k+1}(0) \\ &\times \begin{bmatrix} \bar{A}_k(0) & \bar{B}_k(0) \end{bmatrix} \\ &= \begin{bmatrix} G_{k11} & G_{k12} \\ G_{k12}^T & G_{k22}^T \end{bmatrix} \end{aligned} \quad (21)$$

in which, G_k is a $(2n+md) \times (2n+md)$ matrix, G_{k11} , G_{k12} , and G_{k22} are $(n+md) \times (n+md)$, $(n+md) \times n$, and $n \times n$ matrices, respectively. The definitions of the matrices $\hat{\bar{A}}_k(0)$, $\hat{\bar{B}}_k(0)$, $\hat{P}_{k|k}$ and \hat{Q}_k are

In the third step, the state estimation $\hat{\bar{x}}_{k+1|k+1}$ is calculated by updating $P_{k+1|k}$, $R_{e,k+1}$, $P_{k+1|k+1}$. The definitions of updated formulae $P_{k+1|k}$, $R_{e,k+1}$, $P_{k+1|k+1}$ are as follows:

$$\left\{ \begin{array}{l} P_{k+1|k} = \bar{A}_k(0) \hat{P}_{k|k} \bar{A}_k^T(0) + \hat{\bar{B}}_k(0) \hat{Q}_k \hat{\bar{B}}_k^T(0) \\ R_{e,k+1} = R_{k+1} + \bar{C}_{k+1}(0) P_{k+1|k} \bar{C}_{k+1}^T(0) \\ P_{k+1|k+1} = P_{k+1|k} - P_{k+1|k} \bar{C}_{k+1}^T(0) R_{e,k+1}^{-1} \\ \times \bar{C}_{k+1}(0) P_{k+1|k} \end{array} \right. \quad (23)$$

Then,

$$\begin{aligned} \hat{\bar{x}}_{k+1|k+1} &= \hat{\bar{A}}_k(0) \hat{\bar{x}}_{k|k} + P_{k+1|k+1} \\ &\times \left(P_{k+1|k}^{-1} \left(\bar{A}_k(0) \hat{P}_{k|k} \begin{bmatrix} I_{n+md} & 0_{(n+md) \times n} \end{bmatrix} \right. \right. \\ &\left. \left. + \hat{\bar{B}}_k(0) \hat{Q}_k \hat{\bar{B}}_k^T(0) \begin{bmatrix} -G_{k12}^T \hat{P}_{k|k} & I_n \end{bmatrix} \right) \right) H_{k2} R_{k+1}^{-1} y_{k+1} \\ &- \bar{C}_{k+1}^T(0) R_{k+1}^{-1} \bar{C}_{k+1}(0) \hat{\bar{A}}_k(0) \hat{\bar{x}}_{k|k} \end{aligned} \quad (24)$$

The robust predictive filtering method mentioned above has fixed measurement delay; therefore, it is not applicable for us, but the extrapolation method of the Kalman filter can effectively meet the problem of the predictive step size change. It is similar to Equations (20)–(24), except that the state vector and coefficient matrix of System (11) are used instead of those of System (13). As for the prediction process, we can use

$\hat{A}_k(0)$ to do extrapolation based on the extrapolation method of the Kalman filter.

4.2 | Simulation

The effectiveness of the proposed scheme is verified by simulation. Equation (25) represents a constant velocity (CV) model and Equation (26) represents a constant acceleration (CA) model; they all contain model uncertainty and measurement delay. Here, $T = 0.01$ is the sampling period, $\epsilon \sim N(0, 1)$ is the variable parameter of modelling error, and d indicates different delay frames.

$$\begin{aligned} A &= \begin{bmatrix} 1 & T + 0.05 \cdot \epsilon \\ 0 & 1 \end{bmatrix}, B = \begin{bmatrix} 1 & 0 \\ 0 & 1 \end{bmatrix}, C = [1 \ 0] \\ Q &= \begin{bmatrix} 1.9 & 0 \\ 0 & 0.5 \end{bmatrix}, R = 1 \\ x_0 &= \begin{bmatrix} -158.8 \\ -29.74 \end{bmatrix}, \Pi_0 = \begin{bmatrix} 1 & 0 \\ 0 & 1 \end{bmatrix} \end{aligned} \quad (25)$$

To verify the effectiveness of the proposed scheme, for the same target trajectory, in the case of different prediction step sizes, three different methods are compared: least-squares predictive filtering based on orthogonal polynomials

(LSPF) [19], Kalman predictive filtering (KPF) [20] and our proposed robust predictive filtering method. Figures 8 and 9 shows the prediction result under the CV model, Figures 10 and 11 is under the CA model. The prediction step size is 10 and 100, respectively. The black line represents the real trajectory of the target; the green line, blue line, red line represent predicted trajectory or position estimation error using LSPF, KPF, and our method, respectively. It can be observed that the position estimation error of the proposed method is the smallest whatever the motion model and the prediction step size is.

$$\begin{aligned} A &= \begin{bmatrix} 1 & T + 0.05 \cdot \epsilon & \frac{T^2}{2} + 0.05 \cdot \epsilon \\ 0 & 1 & T + 0.05 \cdot \epsilon \\ 0 & 0 & 1 \end{bmatrix}, B = \begin{bmatrix} 1 & 0 & 0 \\ 0 & 1 & 0 \\ 0 & 0 & 1 \end{bmatrix}, \\ C &= [1 \ 0 \ 0] \\ Q &= \begin{bmatrix} 1.9 & 0 & 0 \\ 0 & 0.5 & 0 \\ 0 & 0 & 0.1 \end{bmatrix}, R = 10 \\ x_0 &= \begin{bmatrix} -33.4919 \\ -0.6527 \\ -0.1687 \end{bmatrix}, \Pi_0 = \begin{bmatrix} 1 & 0 & 0 \\ 0 & 1 & 0 \\ 0 & 0 & 1 \end{bmatrix} \end{aligned} \quad (26)$$

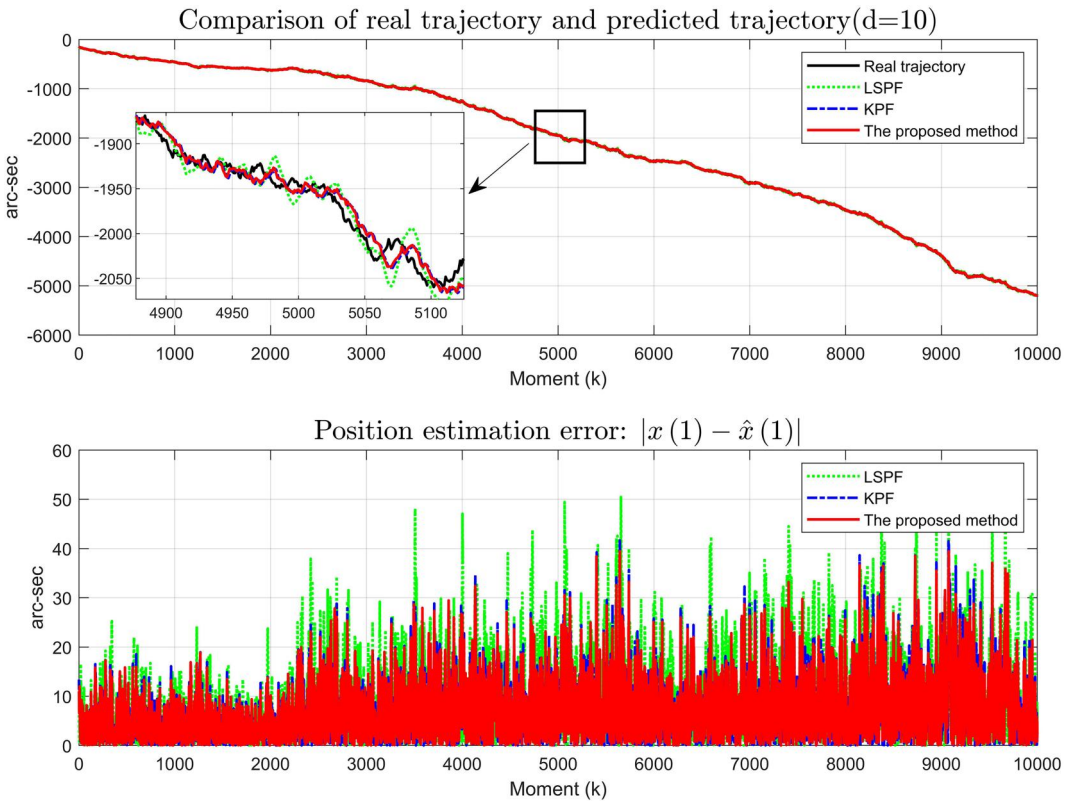


FIGURE 8 Comparisons under the constant velocity model for the three prediction methods ($d = 10$). KPF, Kalman predictive filtering; LSPF, least-squares predictive filtering

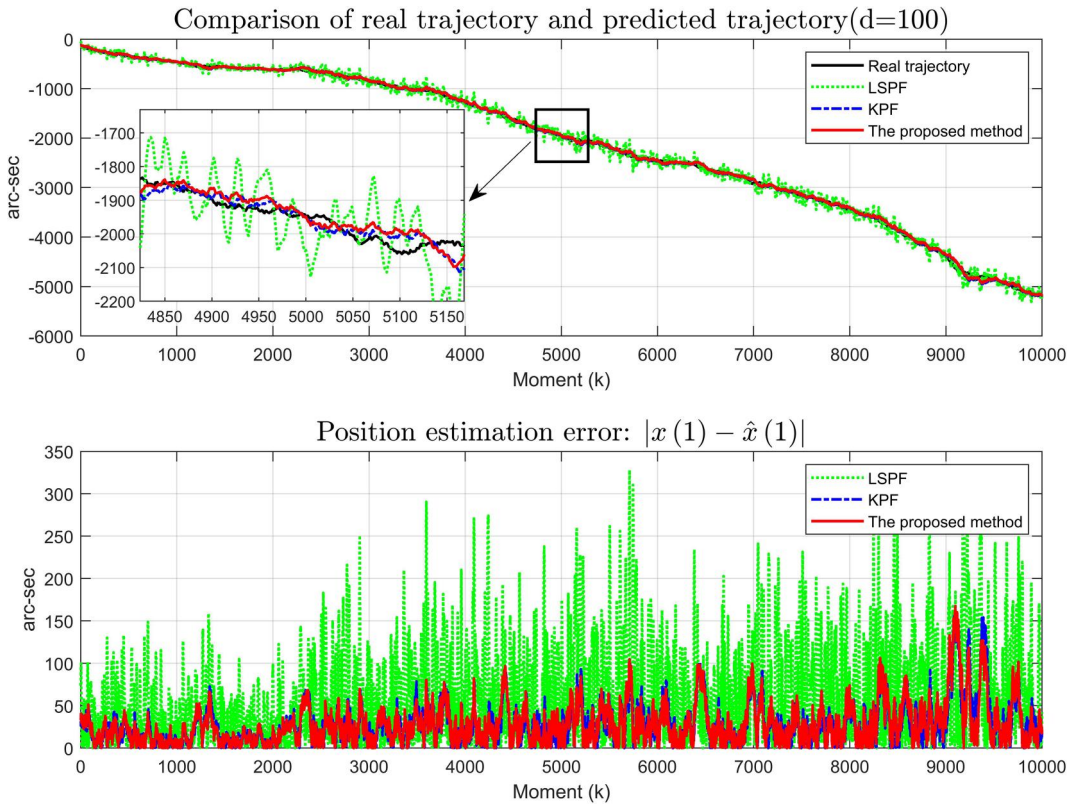


FIGURE 9 Comparisons under the constant velocity model for the three prediction methods ($d = 100$). KPF, Kalman predictive filtering; LSPF, least-squares predictive filtering

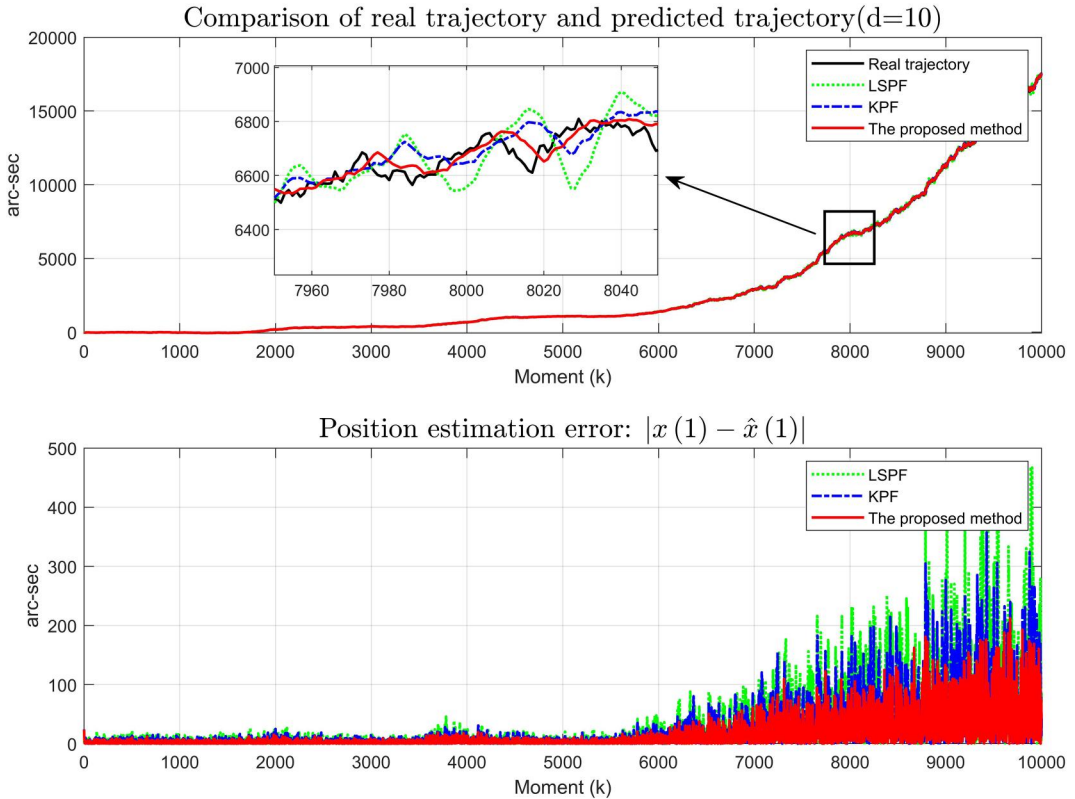


FIGURE 10 Comparisons under the constant acceleration model for the three prediction methods ($d = 10$). KPF, Kalman predictive filtering; LSPF, least-squares predictive filtering

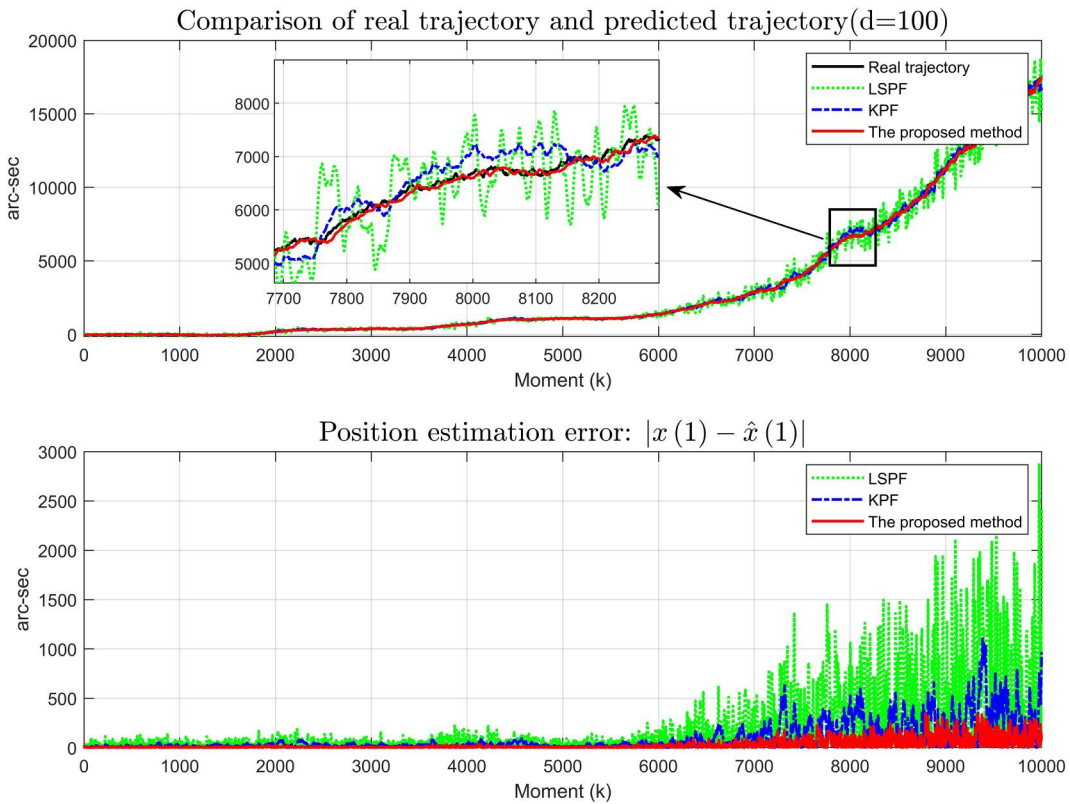


FIGURE 11 Comparisons under the constant acceleration model for the three prediction methods ($d = 100$). KPF, Kalman predictive filtering; LSPF, least-squares predictive filtering

TABLE 1 Mean square error of the position estimation error in the above simulation

Motion model	Prediction step size	Least-squares predictive filtering	Kalman predictive filtering	Our method
CV	10	10.437	8.077	7.725
CV	100	66.438	28.257	27.922
CA	10	34.871	26.354	15.447
CA	100	213.658	94.484	30.187

Abbreviations: CA, constant acceleration; CV, constant velocity.

In addition, Table 1 shows the mean square error (MSE) of the position estimation error in the above simulation. (The definition of MSE is $\sum_{k=1}^n \|x_k - \hat{x}_k\|^2 / n$, here $n = 10000$).

5 | EXPERIMENTAL VERIFICATION OF THE OVERALL SCHEME

In this paper, a real electro-optical tracking system is simulated by a CCD-based dual-fast steering mirror (FSM) experimental platform, and the stable target tracking method of the electro-optical tracking system under full occlusion is comprehensively finished. In this chapter, the CCD-based dual-FSM experimental system is first introduced, and then the controller corresponding to the traditional closed-loop tracking mode is designed according to the actual system. Finally, the occlusion judgement of the image processing unit, and two modes of the

servo control unit are combined to finish the target tracking under the occlusion of uniform speed, uniform acceleration, and sinusoidal signal, respectively. The feasibility of the proposed target tracking method for the electro-optical tracking system under occlusion is verified.

As shown in Figure 12, the experimental system consists of four parts: the first part is called the target motion unit, which is composed of laser, Fast Steering Mirror 1 (FSM1), Motor 1, and the target motion controller. The laser device is used to transmit laser to simulate the target. The target motion controller can give a driving signal according to specific requirements to control the rotation angle of FSM1 through Motor 1 and then make the angle of the laser reflective beam deflect accordingly. This simulates target motion (in this paper, FSM1 is named the target mirror).

The second part is called the occlusion environment unit. There is only one occlusion in this part. When the target mirror

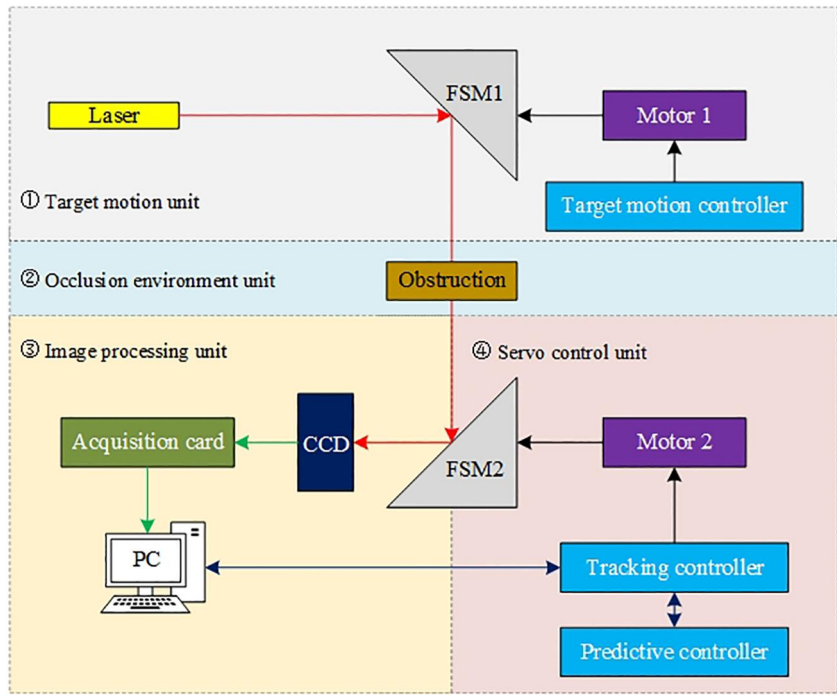


FIGURE 12 Schematic diagram of CCD-based dual-FSM experimental system. FSM, fast steering mirror

is deflected to a certain angle range, the laser reflected by the target mirror will be blocked by the occlusion.

The third part is called the image processing unit. This part is composed of a CCD, an acquisition card, and a personal computer. In this experimental system, the CCD is a camera for detecting the spot target. The acquisition card is used to collect and send the images detected by CCD. The personal computer performs image tracking on the spot target, extracts the LOS error information of the target and the occlusion state information of the target, and transmits it to the servo control unit in the fourth part in real-time.

The fourth part is called the servo control unit. This part is composed of FSM2, Motor 2, the tracking controller, and the predictive controller. The tracking controller uses the target LOS error signal obtained by CCD detection as a tracking error signal to control the deflection angle of FSM2. The deflection direction of FSM2 is reversed to change the optical path of the laser beam so that the spot of the laser always stays at the centre of the CCD target surface (FSM2 is referred to as a tracking mirror in this paper).

In addition, the eddy current position signal sensors are installed on both the target mirror and the tracking mirror, which are used to measure the deflection angle of the fast steering mirrors. In this experimental system, the deflection angle measured by the eddy current sensor on the target mirror can be regarded as the actual position of the target, and the deflection angle measured by the eddy current sensor on the tracking mirror can be regarded as the LOS position of the electro-optical tracking system. Therefore, the position information of the target relative to the electro-optical tracking system is obtained by using the eddy current sensor on the tracking mirror to measure the platform position information

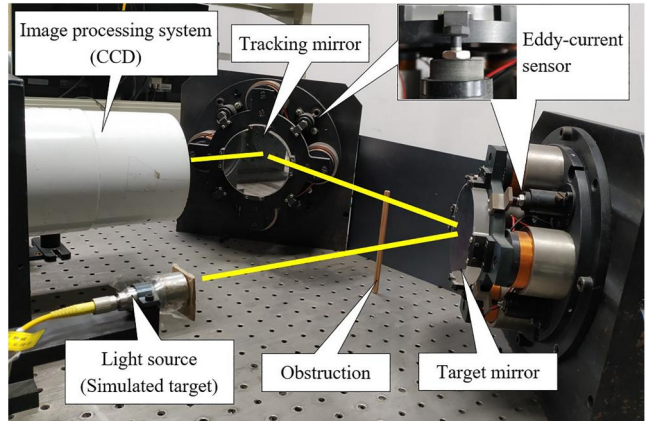


FIGURE 13 Actual experimental system

and by using the target's LOS error information extracted from the CCD image. The actual experimental system is shown in Figure 13.

The specific experimental procedure is described as follows: the target mirror is deflected to a certain extent so that the laser beam undergoes no occlusion stage, the occluding stage, and the stage of leaving the occlusion region, and then the tracking mirror is used to stabilise the tracking laser beam through the LOS error and the occlusion state information so that the laser spot always stays at the centre of the CCD target surface. This experimental system has two axes. Due to the similarity of the two axes, in this paper, only the single axis (Y -axis) is analysed. In addition, the CCD camera used in this experimental system can only obtain greyscale images. The sampling rate of the CCD is 100 Hz, and the time delay is about 0.03 s (3 frames).

The eddy current open-loop controlled object of the tracking mirror is mainly composed of a second-order oscillation link and an inertia link. The inner ring controlled object of the tracking mirror is represented by Equation (27), and its corresponding inner loop controller is given by Equation (28).

$$G(s) = G_{\text{eddy_y}}(s)$$

$$= \frac{7.0126}{\left(\frac{s}{2\pi \cdot 41}\right)^2 + 2 \cdot 0.55 \cdot \frac{s}{2 \cdot \pi \cdot 41} + 1} \cdot \frac{e^{-0.00045s}}{0.005s + 1} \quad (27)$$

$$C_{\text{inner}}(s) = C_{\text{eddy_y}}(s)$$

$$= 13.15 \cdot \frac{(1 + 0.0015s)(1 + 0.0044s)}{s(1 + 0.0017s)(1 + 0.000023s)} \quad (28)$$

The open-loop controlled object of the outer loop and the outer-loop controller is described by Equations (29) and (30):

$$G_{\text{CCD}}(s) = \frac{1.2517}{(0.0106s + 1)(0.008s + 1)} \cdot e^{-0.03s} \quad (29)$$

$$C_{\text{outer}}(s) = C_{\text{CCD}}(s) = 18 \cdot \frac{(1 + 0.0032s)}{s(1 + 0.0017s)(1 + 0.0037s)} \quad (30)$$

$C_f(s)$ is implemented by the Kalman-based prediction algorithm, and derivation of its frequency domain expression can be found in Ref. [21]. In the prediction mode, there is no time delay of the CCD. Therefore, the gain of the outer loop controller can be increased based on the original outer loop controller, and it can be designed as follows:

$$C'_{\text{outer}}(s) = 36 \cdot \frac{(1 + 0.0032s)}{s(1 + 0.0017s)(1 + 0.0037s)} \quad (31)$$

In this experiment, the occlusion situation of the uniform moving target is tracked first. The traditional closed-loop tracking method and the method proposed in this paper are compared. The experiment results are shown in Figure 14 and Figure 15. Figure 14 is an image effect diagram of the conventional closed-loop tracking method when the target is moving at a uniform speed. It can be seen from Figure 14 that the LOS error extracted by the image processing unit is a random quantity. When the spot target exits from the occlusion area, it can be seen that the extraction of the LOS error is failed. Figure 15 shows an image effect using the method proposed in this paper when the target is moving at a uniform speed. As can be seen from Figure 15, even if the spot is occluded, extraction of the LOS error is always kept at the near centre position; when the target exits from the occlusion area, the image processing unit can successfully extract the spot target.

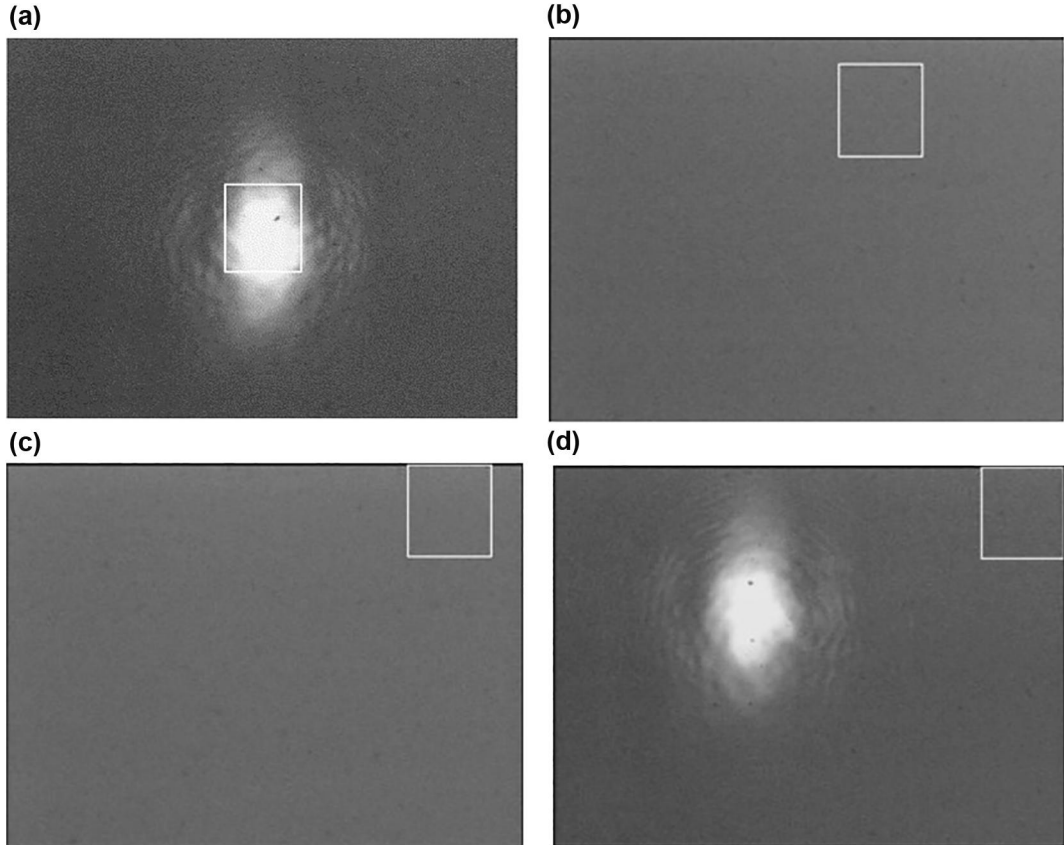


FIGURE 14 Image tracking effect in the constant velocity model (without trajectory prediction): (a) shows the effect before occlusion; (b) and (c) shows the effect in occlusion; (d) shows the effect after occlusion

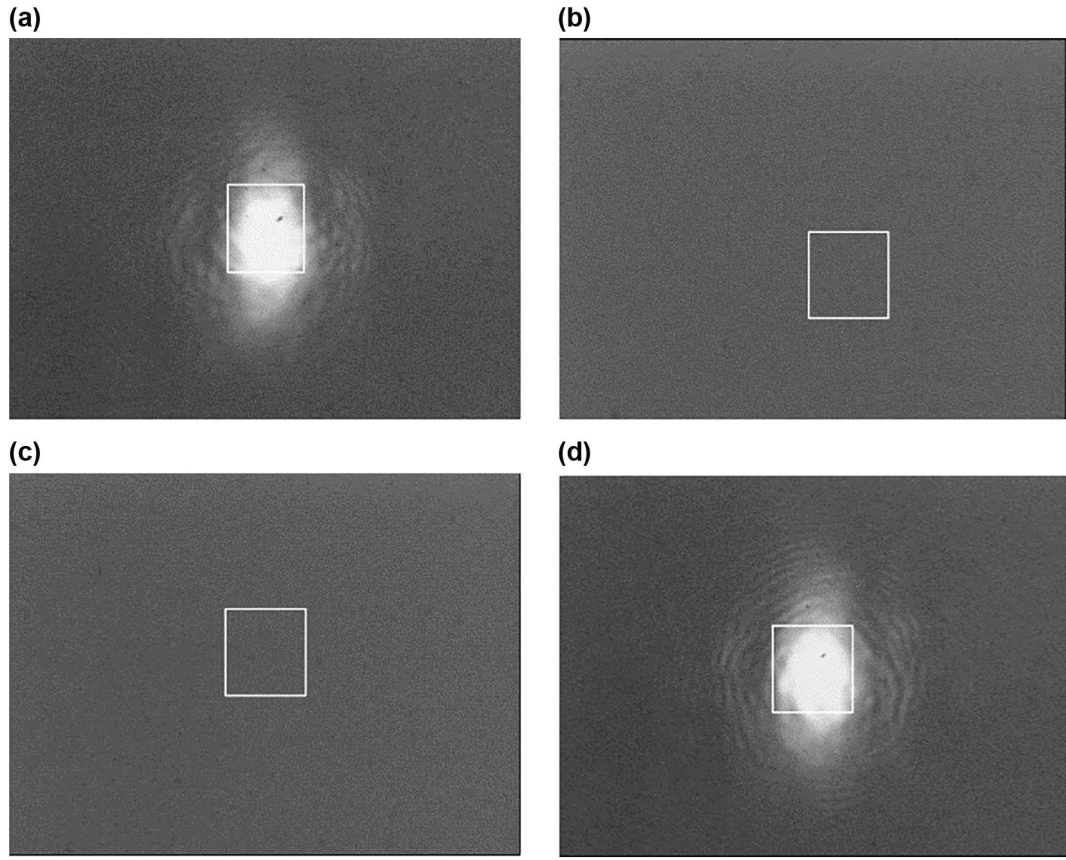


FIGURE 15 Image tracking effect in the constant velocity model (with trajectory prediction): (a) shows the effect before occlusion; (b) and (c) shows the effect in occlusion; (d) shows the effect after occlusion

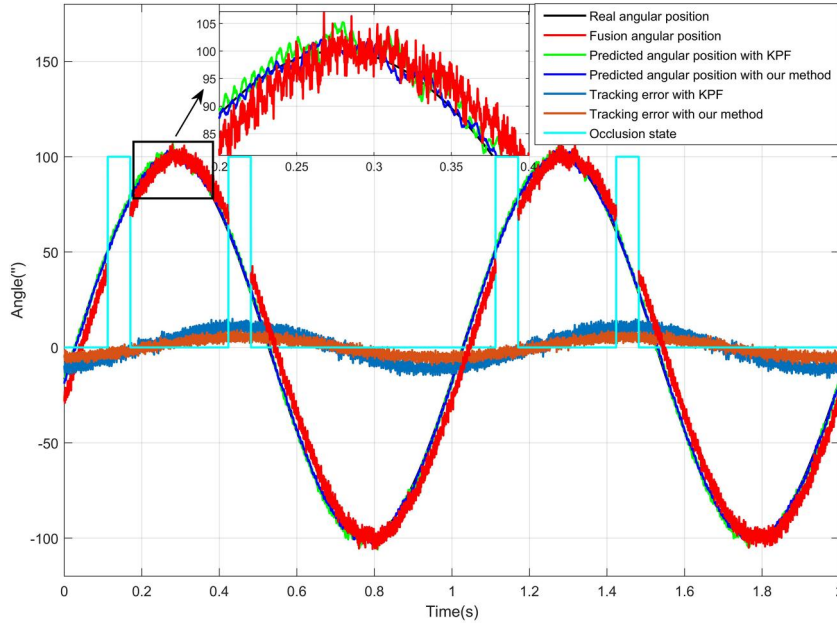
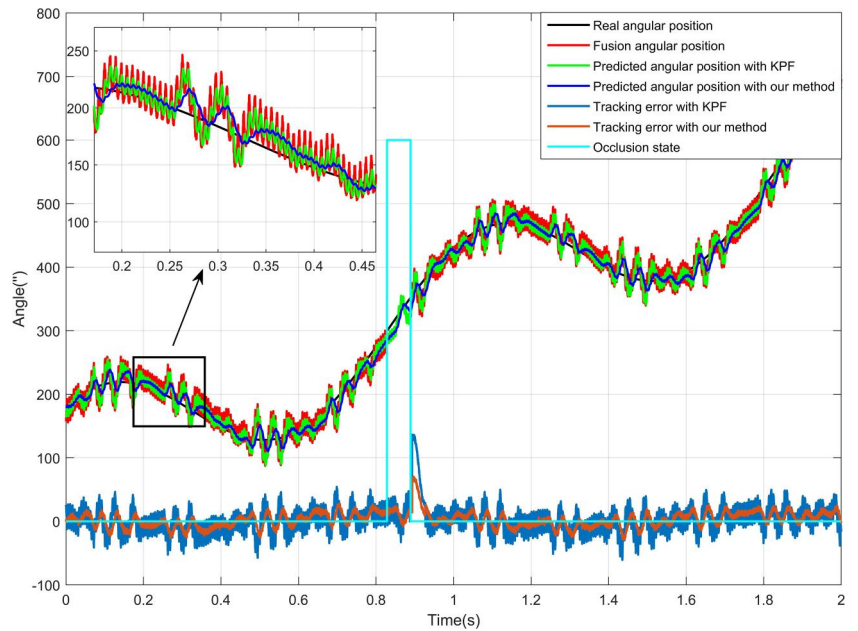


FIGURE 16 Tracking result of the sinusoidal moving target under occlusion. KPF, Kalman predictive filtering

To further demonstrate the effectiveness of this experiment, the data in the experimental system are also given in this paper. In Figure 16, the black line is the real angular position of the target, and the red line represents the fusion angular

position obtained by the LOS error and LOS position. The green line represents the predicted angular position using the KPF method, and the blue line represents the predicted angular position using our proposed method. The dark blue

FIGURE 17 Tracking result of the manoeuvring target under occlusion. KPF, Kalman predictive filtering



line refers to the tracking error using the KPF method, and the brown line refers to the tracking error using our proposed method. The cyan line indicates the occlusion state of the target. As can be seen from Figure 16, when the target is occluded, the tracking method proposed in this paper is used to track the target continuously, and the tracking error does not change greatly, so the feasibility and the effectiveness of the proposed method can be verified. Moreover, the tracking error of our method is also less than the KPF method.

Besides, Figure 17 shows that when facing a manoeuvring target and occlusion problem, the method proposed in this paper can also be used to track the target effectively. Although the tracking error will have a chattering after occlusion, compared to the KPF method, our method can also reduce it.

6 | CONCLUSIONS

In this paper, in terms of the target tracking problem of the electro-optical tracking system under occlusion, a dual-channel anti-occlusion scheme based on image processing and trajectory prediction is proposed. Next, according to the most critical occlusion judgement method in this scheme, an occlusion judgement method based on the improved Bhattacharyya coefficient with background weighting is proposed. The anti-interference ability of this method for the occluder with similar background pixels and the improvement of judgement speed is verified by comparison experiments. Then, considering the time delay, model uncertainty, and variable prediction step size, the prediction accuracy is improved by using robust predictive filtering in the prediction model. Finally, the feasibility and effectiveness of the proposed scheme are comprehensively verified on the CCD-based dual fast steering mirror platform. However, the innovation of this paper is mainly reflected in the ideas and the feasibility

verification in the early stage. When the target moves linearly in a 3-dimensional space, its angular motion for the servo system is not necessarily linear, while there is a non-linear transformation relationship, so the non-linear filtering and prediction need to be considered later. Second, for complex scenarios, target scales, illumination, and rotation changes, there are still some shortcomings in the proposed target occlusion judgement method based on the improved Bhattacharyya coefficient with background weighting, so further research is necessary.

ACKNOWLEDGEMENT

This work was supported in part by the National Natural Science Foundation of China (No.61733012, No.61905253).

CONFLICT OF INTEREST

To the best of our knowledge, the named authors have no conflict of interest, financial or otherwise.

DATA AVAILABILITY STATEMENT

The data are openly available in a public repository that issues datasets with DOIs.

ORCID

Wenqiang Xia <https://orcid.org/0000-0002-0788-3892>

Yao Mao <https://orcid.org/0000-0003-1785-2018>

REFERENCES

1. Berg, R.: Estimation and prediction for maneuvering target trajectories. *IEEE Trans. Automat. Control*. 28(3), 294–304 (1983)
2. Han, S.K., et al.: Linear recursive passive target tracking filter for cooperative sea-skimming anti-ship missiles. *IET Radar, Sonar Navig.* 8(7), 805–814 (2014)
3. Tian, Y., Guan, T., Wang, C.: Real-time occlusion handling in augmented reality based on an object tracking approach. *Sensors*. 10(4), 2885–2900 (2010)

4. Memon, S., et al.: Multi-scan smoothing for tracking manoeuvering target trajectory in heavy cluttered environment. *IET Radar, Sonar Navig.* 11(12), 1815–1821 (2017)
5. Queirós, S., et al.: MITT: medical image tracking toolbox. *IEEE Trans. Med. Imag.* 37(11), 2547–2557 (2018)
6. Kim, J.: 3D path planner of an autonomous underwater vehicle to track an emitter using frequency and azimuth+elevation angle measurements. *IET Radar, Sonar Navig.* 14(8), 1236–1243 (2020)
7. Li, Z., et al.: Improved mean shift algorithm for multiple occlusion target tracking. *Opt. Eng.* 47(8), 086402 (2008)
8. Mao, J., et al.: Research on realizing the 3D occlusion tracking location method of fish's school target. *Neurocomputing.* 214, 61–79 (2016)
9. Jianguang, M.: The basic technologies of the acquisition, tracking and pointing systems. *Opto-Electronic Eng.* 16(3), 1–42 (1989)
10. Comaniciu, D., Ramesh, V., Meer, P.: Kernel-based object tracking. *IEEE Trans. Pattern Anal. Mach. Intell.* 25(5), 564–577 (2003)
11. Wu, B., Nevatia, R.: Detection and tracking of multiple, partially occluded humans by Bayesian combination of edgelet based part detectors. *Int. J. Comput. Vis.* 75(2), 247–266 (2007)
12. Huang, Y., Ma, J., Fu, C.: Application of forecast of moving target velocity in electro-optical tracking control system. *Infrared Laser Eng.* 33(5), 477–481 (2004)
13. Kalman, R.E.: A new approach to linear filtering and prediction problems. *J. Basic Eng.* 82(1), 35–45 (1960)
14. Ehrman, L., Lanterman, A.: Extended Kalman filter for estimating aircraft orientation from velocity measurements. *IET Radar, Sonar Navig.* 2(1), 12–16 (2008)
15. Julier, S.J., Uhlmann, J.K.: New extension of the Kalman filter to nonlinear systems. vol. 3068, pp. 182–193. International Society for Optics and Photonics. (1997)
16. Isard, M., Blake, A.: Condensation conditional density propagation for visual tracking. *Int. J. Comput. Vis.* 29(1), 5–28 (1998)
17. Bhattacharyya, A.: On a measure of divergence between two statistical populations defined by their probability distributions. *Bull. Calcutta Math. Soc.* 35, 99–109 (1943)
18. Liu, H., Zhou, T.: Robust state estimation for uncertain linear systems with random parametric uncertainties. *IEEE Trans. Automat. Control.* 60(1), 012202 (2017)
19. Ding, K., Ou, J., Zhao, C.: Methods of the least-squares orthogonal distance fitting. *Sci. Surv. Mapp.* 32(2), 18–19 (2007)
20. He, Q., et al.: An acceleration feed-forward control method based on fusion of model output and sensor data. *Sensor Actuator Phys.* 284, 186–193 (2018)
21. Kailath, T., Sayed, A.H., Hassibi, B.: *Linear estimation*. Prentice Hall, NJ (2000)

How to cite this article: Xia, W., et al.: A target anti-occlusion method based on image processing and trajectory prediction in electro-optical tracking system. *IET Radar Sonar Navig.* 1–16 (2022). <https://doi.org/10.1049/rsn2.12235>